Particle Accelerators
1983 Vol. 13 pp. 179–198
0031-2460/83/1303/0179$06.50/0

Gordon and Breach, Science Publishers, Inc.
Printed in the United States of America

MODE-COUPLING THEORY AND BUNCH LENGTHENING IN SPEAR II

TOSHIO SUZUKI, YONGHO CHIN† AND KOHTARO SATOH

National Laboratory for High Energy Physics
Oho-machi, Tsukuba-gun, Ibaraki-ken, 305, Japan

(Received November 30, 1982; in final form February 1, 1983)

A mode-coupling theory of bunched-beam instabilities is developed for a Gaussian bunch. The theory converts Sacherer's integral equation with mode coupling into a matrix eigenvalue problem. The present theory assumes well-defined azimuthal modes and takes into account radial modes which are expressed as superpositions of orthogonal functions. The theory is applied to bunch lengthening observed at SPEAR II. The theory explains qualitative features of the experimental results fairly well, but quantitative agreement is not too good. This is ascribed to our insufficient knowledge of the coupling impedance of SPEAR II or to the possibility that such effects as radiation damping and quantum excitation should be included.

1. INTRODUCTION

Sacherer's general theories[1,2] explain bunched-beam instabilities systematically. These are based on the Vlasov equation and use integral equations known as Sacherer's equations. First,[1] Sacherer dealt with a case where beam intensity is relatively low and azimuthal modes such as the dipole mode, quadrupole mode, etc. are well separated. In this theory, the coupled-bunch instabilities are explained. However, a single bunch is shown to be stable in this theory except for the relatively weak Robinson instability[3] and strong single-bunch instabilities such as microwave instability in proton beams and anomalous bunch lengthening in electron beams cannot be explained.

Later,[2] he extended his theory to a case where the beam intensity is high and two different azimuthal modes couple to give rise to strong instability. He showed that this theory gives results numerically similar to those obtained by the Laslett-Neil-Sessler (LNS) criterion[4] (sometimes referred to as the Keil-Schnell criterion) widely used to explain microwave instabilities.

Chao and Gareyte[5] developed a mode-coupling theory using the waterbag model. They applied the theory phenomenologically to the bunch lengthening observed at SPEAR II and derived a scaling law which fitted the experimental data quite well. Chao[6] recently calculated the threshold of bunch lengthening in SPEAR II by the waterbag model and found that it was caused by the coupling between dipole and quadrupole modes. At present, the microwave instability in proton beams and the anomalous bunch lengthening in electron beams are considered to be the same phenomenon, both being explained by the mode-coupling theory or by a criterion something like the LNS criterion. In fact, the bunch-lengthening data at SPEAR II are qualitatively explained by the LNS criterion[7] or by the scaling law of Chao and Gareyte. However, no quantitative calculation using mode-coupling theory has been done by using a Gaussian bunch distribution relevant for an electron beam.

† On leave from Department of Physics, The University of Tokyo, Bunkyo-ku, Tokyo, 113.

Recently, Satoh[8] developed a mode-coupling theory for Gaussian and parabolic bunches. He used Sacherer's integral equation in the frequency domain and expanded a perturbed distribution function in terms of linearly independent functions. In this theory, the eigenfrequencies of coherent oscillations can be obtained by solving determinant equations. Satoh and Chin[9] applied this theory to the transverse fast instability and explained the experimental results at PEP and PETRA. Zotter[10] used a mode-coupling theory for a Gaussian bunch using one radial mode for each azimuthal mode to study the transverse fast instability.

Here we develop a new formalism of mode-coupling theory for a Gaussian bunch. In this formalism, well-defined azimuthal modes are assumed and radial mode functions are expressed as superpositions of orthogonal functions. The method is an extension of the theory of Besnier,[11] who applied it to solve Sacherer's integral equations without mode coupling. The present theory is similar to Satoh's and the relation between the two theories is explained in the Appendix. In contrast to Satoh's theory, the present theory is formulated as a matrix eigenvalue problem and is better suited for computer calculation. The eigenfunctions can also be obtained more easily.

The theory is applied to the bunch lengthening observed at SPEAR II. The theory explains some qualitative features of the data fairly well, but quantitative agreement between the theory and the experiment is not too good. The theory predicts threshold currents of anomalous bunch lengthening which are larger than the experimental data by several factors. The disagreement is ascribed to our insufficient knowledge of the coupling impedance or to a possibility that such effects as radiation damping and quantum excitation should be included in the theory. Section 2 is devoted to the development of the mode-coupling theory. In Section 3, the theory is applied to the bunch lengthening in SPEAR II. Section 4 gives conclusions. In the Appendix, the relation between the present theory and Satoh's one is explained.

2. MODE-COUPLING THEORY

In this section, we develop a new formalism of mode-coupling theory. We first derive Sacherer's integral Eq. (2.20) for the case of mode coupling. The derivation is based on Ref. (12). We start from the Vlasov equation

$$\frac{\partial \psi}{\partial \theta_L} + \theta' \frac{\partial \psi}{\partial \theta} + \epsilon' \frac{\partial \psi}{\partial \epsilon} = 0, \tag{2.1}$$

where ψ is a particle distribution function, θ_L is the azimuthal angle around the machine circumference, θ is the longitudinal angular position of a particle with respect to the bunch center and ϵ is the energy deviation from the synchronous value. The primes on θ and ϵ denote differentiation with respect to θ_L. The equations of synchrotron oscillations are

$$\omega_0 \frac{d\theta}{d\theta_L} = -k_0 \epsilon, \tag{2.2}$$

$$\omega_0 \frac{d\epsilon}{d\theta_L} = \frac{\Omega_S{}^2}{k_0} \theta + \frac{eV(\theta, t)}{T}, \tag{2.3}$$

where

$$k_0 = \frac{\alpha\omega_0}{E} \tag{2.4}$$

and ω_0 is the revolution frequency, Ω_s is the synchrotron-oscillation frequency including the Laslett tune shift, T is the revolution period $(= 2\pi/\omega_0)$, E is the beam energy, α is the momentum-compaction factor, $eV(\theta, t)$ is the energy gain per revolution for a particle at longitudinal position θ relative to the bunch center and t is the time. The quantities θ, θ_L and t are related by $\theta_L = \omega_0 t + \theta$.

Equation (2.1), is then transformed from Cartesian coordinates (θ, ϵ) to polar coordinates (r, ϕ) defined by

$$\theta = r\cos\phi, \tag{2.5}$$

$$\epsilon = \frac{\Omega_s}{k_0} r \sin\phi. \tag{2.6}$$

The use of action-angle variables is more appropriate, as explained in Ref. (12), but polar coordinates are used here according to Sacherer[1] for simplicity of presentation. The distribution function ψ is decomposed into an unperturbed part $\psi_0(r)$, which is a function of r only, and a perturbed part $f(r, \phi)$ as

$$\begin{aligned}\psi(r, \phi, \theta_L) &= \psi_0(r) + f(r,\phi)\exp\left(-i\frac{\Omega}{\omega_0}\theta_L\right)\\ &= \psi_0(r) + f(r,\phi)\exp\left(-i\Omega t - i\frac{\Omega}{\omega_0}\theta\right).\end{aligned} \tag{2.7}$$

The function ψ_0 is normalized as

$$\iint \psi_0(\theta, \epsilon)\, d\theta\, d\epsilon = Ne, \tag{2.8}$$

or

$$\iint \psi_0(r)\, r dr\, d\phi = \frac{Ne\alpha\omega_0}{\Omega_S E}, \tag{2.9}$$

where N is the number of electrons in a bunch and the perturbed part has zero normalization. With Eqs. (2.2), (2.3) and (2.7), the Vlasov equation (2.1) is expressed in terms of the polar coordinates r and ϕ as

$$-i\Omega\psi + \Omega_S\frac{\partial\psi}{\partial\phi} + \frac{eV(\theta, t)}{T}\frac{k_0}{\Omega_S}\sin\phi\frac{d\psi_0}{dr} = 0, \tag{2.10}$$

where only terms linear in ψ are retained.

Since the impedance or the wake function picks up a current signal in time, we express the beam current as

$$i(t) = \omega_0 \sum_{p=-\infty}^{\infty} \tilde{\rho}\left(p + \frac{\Omega}{\omega_0}\right) \exp[-i(p\omega_0 + \Omega)t], \tag{2.11}$$

where the Fourier transform of the longitudinal charge distribution is given by

$$\tilde{\rho}\left(p + \frac{\Omega}{\omega_0}\right) = \frac{1}{2\pi}\frac{\Omega_s}{k_0} \int\int f(r, \phi) \exp\left[-i\left(p + \frac{\Omega}{\omega_0}\right) r\cos\phi\right] rdr\, d\phi. \tag{2.12}$$

Since with impedance $Z(\omega)$,[12]

$$eV(\theta, t) = -e\omega_0 \sum_{p=-\infty}^{\infty} \tilde{\rho}\left(p + \frac{\Omega}{\omega_0}\right) Z(p\omega_0 + \Omega) \times \exp\left[i\left(p + \frac{\Omega}{\omega_0}\right)\theta - i\Omega t\right], \tag{2.13}$$

we obtain

$$\left(-i\Omega + \Omega_s \frac{\partial}{\partial\phi}\right) f(r, \phi) = \frac{e\omega_0}{T}\frac{k_0}{\Omega_s} \sin\phi \frac{d\psi_0}{dr} \times \sum_{p=-\infty}^{\infty} \tilde{\rho}\left(p + \frac{\Omega}{\omega_0}\right) Z(p\omega_0 + \Omega) \exp\left[i\left(p + \frac{\Omega}{\omega_0}\right) r\cos\phi\right]. \tag{2.14}$$

The function $f(r, \phi)$ is periodic with period 2π, and so we multiply both sides of Eq. (2.14) by $\exp(-i\lambda\phi)$, where

$$\lambda = \frac{\Omega}{\Omega_s}, \tag{2.15}$$

integrate with ϕ and obtain

$$f(r, \phi) = \frac{e\omega_0 k_0}{T\Omega_s^2}\frac{d\psi_0}{dr} \exp(i\lambda\phi) \frac{1}{\exp(-2\pi i\lambda) - 1} \times \sum_{p=-\infty}^{\infty} \tilde{\rho}\left(p + \frac{\Omega}{\omega_0}\right) \times Z(p\omega_0 + \Omega) \int_{\phi}^{\phi+2\pi} \exp(-i\lambda\phi') \sin\phi' \exp\left[i\left(p + \frac{\Omega}{\omega_0}\right) r\cos\phi'\right] d\phi'. \tag{2.16}$$

Performing the integral, we obtain

$$f(r, \phi) = i\frac{e\omega_0 k_0}{T\Omega_s^2}\frac{1}{r}\frac{d\psi_0}{dr} \sum_{p=-\infty}^{\infty} \frac{Z(p\omega_0 + \Omega)}{p + \Omega/\omega_0} \times \tilde{\rho}\left(p + \frac{\Omega}{\omega_0}\right) \sum_{m=-\infty}^{\infty} \frac{m}{m - \lambda} i^m J_m\left(\left(p + \frac{\Omega}{\omega_0}\right) r\right) \exp(im\phi). \tag{2.17}$$

Now, since the function $f(r, \phi)$ is periodic, we expand it in Fourier series

$$f(r, \phi) = \sum_{m=-\infty}^{\infty} R_m(r) \exp(im\phi). \tag{2.18}$$

Then, from Eq. (2.12), we obtain

$$\tilde{\rho}\left(p + \frac{\Omega}{\omega_0}\right) = \frac{\Omega_s}{k_0} \sum_{m=-\infty}^{\infty} i^{-m} \int_0^{\infty} R_m(r)\, J_m\left(\left(p + \frac{\Omega}{\omega_0}\right) r\right) r dr. \tag{2.19}$$

From Eqs. (2.17) and (2.19), we obtain

$$\frac{m - \lambda}{m} R_m(r) = i \frac{e\omega_0}{T\Omega_s} \frac{1}{r} \frac{d\psi_0}{dr} \sum_{p=-\infty}^{\infty} \frac{Z(p\omega_0 + \Omega)}{p + \Omega/\omega_0} \times J_m\left(\left(p + \frac{\Omega}{\omega_0}\right) r\right) i^m \sum_{n=-\infty}^{\infty} i^{-n}$$
$$\times \int_0^{\infty} R_n(r') J_n\left(\left(p + \frac{\Omega}{\omega_0}\right) r'\right) r' dr'. \tag{2.20}$$

Equation (2.20) is Sacherer's integral equation with mode coupling.

We solve Eq. (2.20) for $R_m(r)$ by expanding the function $R_m(r)$ in terms of orthogonal functions. This method is due to Besnier,[11] who used it for solving Sacherer's equation without mode coupling. Firstly, we notice from Eq. (2.20) that

$$\frac{m + \lambda}{m} R_{-m}(r) = \frac{m - \lambda}{m} R_m(r), \tag{2.21}$$

and the functional dependence of $R_m(r)$ for positive and negative m is the same except for constant factors. Thus we expand $R_m(r)$ as

$$R_m(r) = W(r) \sum_{k=0}^{\infty} a_k^{(m)} f_k^{(|m|)}(r), \tag{2.22}$$

where the $f_k^{(|m|)}(r)$ are appropriate orthogonal functions to be chosen later, the $a_k^{(m)}$ are constant coefficients and the weight function $W(r)$ is defined as

$$W(r) = C \frac{1}{r} \frac{d\psi_0}{dr}. \tag{2.23}$$

Here C is a normalization constant to be determined later in Eq. (2.37). We assume an orthogonality relation

$$\int_0^{\infty} W(r) f_k^{(|m|)}(r) f_l^{(|m|)}(r)\, r dr = \delta_{kl}. \tag{2.24}$$

Inserting Eq. (2.22) into Eq. (2.20), multiplying $f_k^{(|m|)}(r)$ and integrating, we obtain the matrix eigenvalue equation

$$\frac{m-\lambda}{m} a_h^{(m)} = i \frac{e\omega_0}{T\Omega_s C} \sum_{n=-\infty}^{\infty} \sum_{l=0}^{\infty} M_{nl}^{mh} a_l^{(n)}, \tag{2.25}$$

where

$$M_{nl}^{mh} = \sum_{p=-\infty}^{\infty} \frac{Z(p\omega_0 + \Omega)}{p + \Omega/\omega_0} i^{m-n} I_{mh}\left(p + \frac{\Omega}{\omega_0}\right) I_{nl}\left(p + \frac{\Omega}{\omega_0}\right), \tag{2.26}$$

and

$$I_{nl}\left(p + \frac{\Omega}{\omega_0}\right) = \int_0^{\infty} W(r) f_l^{(|m|)}(r) J_n\left(\left(p + \frac{\Omega}{\omega_0}\right) r\right) r dr. \tag{2.27}$$

We now turn to the problem of determining the orthogonal functions $\{f_k^{(|m|)}(r)\}$. The unperturbed distribution function $\psi_0(r)$ is normalized as in Eq. (2.8) or (2.9). Since the stationary distribution is Gaussian for an electron bunch,

$$\psi_0(r) = \frac{Ne\alpha}{2\pi\nu_S E\sigma_\theta^2} \exp\left(-\frac{r^2}{2\sigma_\theta^2}\right), \tag{2.28}$$

where σ_θ is the rms bunch length divided by the average radius of the storage ring and ν_s is the synchrotron tune given by Ω_s/ω_0. Then the weight function (2.23) is

$$W(r) = C' \exp\left(-\frac{r^2}{2\sigma_\theta^2}\right), \tag{2.29}$$

where

$$C' = -C \frac{Ne\alpha}{2\pi\nu_S E\sigma_\theta^4}. \tag{2.30}$$

With this weight function, the orthogonality relation (2.24) becomes

$$C'\sigma_\theta^2 \int_0^{\infty} \exp(-x) f_k^{(|m|)}(x) f_l^{(|m|)}(x)\, dx = \delta_{kl}, \tag{2.31}$$

where

$$x = \frac{r^2}{2\sigma_\theta^2}. \tag{2.32}$$

As we see from Eq. (2.20), $R_m(r)$ behaves like r^m as r approaches zero, so that we put

$$f_k^{(|m|)}(x) = x^{\frac{|m|}{2}} g_k^{(|m|)}(x). \tag{2.33}$$

Then Eq. (2.31) becomes

$$C'\sigma_\theta^2 \int_0^\infty \exp(-x)x^{|m|}g_k^{(|m|)}(x)g_l^{(|m|)}(x)\,dx = \delta_{kl}. \tag{2.34}$$

Equation (2.34) suggests the generalized Laguerre polynomials $\{L_k^{(|m|)}\}$, whose orthogonality relation is given by formula 22.2.12 of Ref. 13 as

$$\int_0^\infty \exp(-x)x^{|m|}L_k^{(|m|)}(x)L_l^{(|m|)}(x)\,dx = \frac{(|m| + l)!}{l!}\,\delta_{kl}. \tag{2.35}$$

Thus we can choose

$$g_l^{(|m|)}(x) = \left(\frac{l!}{(|m| + l)!C'\sigma_\theta^2}\right)^{1/2} L_l^{(|m|)}(x). \tag{2.36}$$

We choose $C'\sigma_\theta^2 = 1$ so that

$$C = -\frac{2\pi\nu_s E\sigma_\theta^2}{Ne\alpha}, \tag{2.37}$$

and

$$f_l^{(|m|)}(r) = \left(\frac{l!}{(|m| + l)!}\right)^{1/2}\left(\frac{r}{\sqrt{2}\sigma_\theta}\right)^{|m|} L_l^{(|m|)}\left(\frac{r^2}{2\sigma_\theta^2}\right). \tag{2.38}$$

We can now evaluate the matrix elements (2.26). We first show results for positive n. The result for negative n will be given later in Eq. (2.45). For this we evaluate $I_{nl}(p')$ given by Eq. (2.27).

$$I_{nl}(p') = C' \int_0^\infty \exp\left(-\frac{r^2}{2\sigma_\theta^2}\right)\left(\frac{l!}{(n + l)!}\right)^{1/2}\left(\frac{r}{\sqrt{2}\sigma_\theta}\right)^n L_l^{(n)}\left(\frac{r^2}{2\sigma_\theta^2}\right)J_n(p'r)\,r\,dr. \tag{2.39}$$

Changing the variable from r to x as given by Eq. (2.32), we obtain

$$I_{nl}(p') = \left(\frac{l!}{(n + l)!}\right)^{1/2} \int_0^\infty \exp(-x)x^{n/2}L_l^{(n)}(x)J_n(\sqrt{2}\sigma_\theta p'\sqrt{x})\,dx. \tag{2.40}$$

We put

$$\zeta = \sqrt{2}\sigma_\theta p', \tag{2.41}$$

and use Rodrigues' formula for the generalized Laguerre function (formula 22.11.6 of Ref. 13)

$$L_l^{(n)}(x) = \frac{\exp(x)x^{-n}}{l!}\frac{d^l}{dx^l}(\exp(-x)x^{n+l}), \tag{2.42}$$

and the power-series expansion of the Bessel function (formula 9.1.10 of Ref. 13)

$$J_n(\zeta\sqrt{x}) = \frac{\zeta^n x^{n/2}}{2^n} \sum_{h=0}^{\infty} \frac{(-1)^h \zeta^{2h} x^h}{4^h h!(n+h)!} \tag{2.43}$$

Inserting Eqs. (2.42) and (2.43) into (2.40) and integrating by parts n times, we obtain

$$I_{nl}(p') = \frac{1}{((n+l)!l!)^{1/2}} \left(\frac{\zeta}{2}\right)^{n+2l} \exp\left(-\frac{\zeta^2}{4}\right). \tag{2.44}$$

For $n < 0$, we obtain

$$I_{-nl}(p') = (-1)^n I_{nl}(p'). \tag{2.45}$$

Since the matrix elements are now calculated, we can solve the matrix equation (2.25) and look at the possibility of instability (complex eigenvalue λ). However, both positive and negative azimuthal modes m appear in the matrix equation, and we can combine them to reduce the matrix size. We first note from Eq. (2.26) that

$$M_{nl}^{-mh} = M^{mh}_{-nl} = M^{mh}_{nl}, \tag{2.46}$$

and by putting

$$b_h^{(m)} = a_h^{(m)} + a_h^{(-m)} \qquad (m > 0), \tag{2.47}$$

we obtain from Eq. (2.25) the matrix equation

$$\frac{m^2 - \lambda^2}{2m^2} b_h^{(m)} = i\frac{e\omega_0}{T\Omega_s C} \sum_{n=1}^{\infty} \sum_{l=0}^{\infty} M_{nl}^{mh} b_l^{(n)} \qquad (m > 0). \tag{2.48}$$

We replace C from Eq. (2.37) and if we use the scaling parameter ξ of Chao and Gareyte[5]

$$\xi = \frac{\alpha I}{\nu_s^2 E}, \tag{2.49}$$

we obtain

$$\frac{m^2 - \lambda^2}{2m^2} b_h^{(m)} = -i\frac{e\xi}{2\pi\sigma_\theta^2} \sum_{n=1}^{\infty} \sum_{l=0}^{\infty} M_{nl}^{mh} b_l^{(n)}. \tag{2.50}$$

Equation (2.50) is reformulated into a form more convenient for computer calculation

$$\lambda^2 b_h^{(m)} = \sum_{n=1}^{\infty} \sum_{l=0}^{\infty} A_{nl}^{mh} b_l^{(n)}, \tag{2.51}$$

where the matrix element is

$$A_{nl}^{mh} = m^2\, \delta_{mn}\, \delta_{hl} + i\frac{m^2 \xi e}{\pi\sigma_\theta^2} M_{nl}^{mh}. \tag{2.52}$$

The condition of stability is that the eigenvalue λ^2 is real and positive.

3. BUNCH LENGTHENING IN SPEAR II

The mode-coupling theory developed in Section 2 is applied to the bunch lengthening observed at SPEAR II because extensive data and some knowledge of the coupling impedance of the SPEAR ring are available. Wilson et al.[14] have given detailed experimental data of bunch lengthening at SPEAR II. They also gave the real part of the coupling impedance of SPEAR II by using the frequency dependence suggested by the scaling law of Chao and Gareyte[5] and by fitting the resulting form of the impedance to the experimental data of higher-order mode loss. The imaginary part of the coupling impedance is given by Bane and Wilson[15] by using the Hilbert transformation.

Recently Siemann[16] used the above impedance to obtain the wake function of SPEAR II and applied this wake function to the time-domain simulation of the bunch lengthening at SPEAR II. He took into account Robinson damping, radiation damping and quantum excitation and obtained results which fitted to the experimental data quite well.

Impedance of Wilson et al.

With the coupling impedance of Wilson et al. we calculate the threshold of bunch lengthening by using the matrix formalism developed in Section 2. The results are shown in Fig. 1(a). In the figure, a scaling parameter G defined by Wilson[17] as

$$G = \frac{eT^2\xi}{(2\pi)^{5/2}}, \tag{3.1}$$

where T is the revolution period and ξ is given by Eq. (2.49), is shown in units of (picosecond)^2/ohm. The solid curve shows the result when four azimuthal ($m \leqq 4$) and five radial ($l \leqq 4$) modes are included. The dashed curve shows the result when two azimuthal ($m \leqq 2$) and five radial ($l \leqq 4$) modes are included. The dot-dash curve shows the result when two azimuthal modes ($m \leqq 2$) and only one radial ($l = 0$) mode for each azimuthal mode are included. The triangles show the experimental data which are taken from Refs. 14 and 17. A calculation using four azimuthal ($m \leqq 4$) and ten radial ($l \leqq 9$) modes has also been done, but the result is almost the same with the case where four azimuthal ($m \leqq 4$) and five radial ($l \leqq 4$) modes are included.

The calculated curves are about three to four times as large as the experimental data at short bunch and become still larger at larger bunch length. Up to $\sigma = 4$ cm, the calculated results are the coupling between $m = 1$ (dipole) and $m = 2$ (quadrupole) modes, but at $\sigma = 5$ cm, the calculated result is the coupling between $m = 2$ (quadrupole) and $m = 3$ (sextupole) modes. These are seen by looking at the real parts of the eigenvalues. Figure 1(b) shows the result for higher-order mode losses. The loss parameter k defined Ref. 14 is plotted in units of volt/pico-Coulomb. The solid curve shows the calculation by using the impedance of Wilson et al. and the dashed curve represents the experimental results. The experimental data are represented by the fit

$$k = 50\{\sigma(\mathrm{cm})\}^{-1.21}(\mathrm{V/pC}). \tag{3.2}$$

We see from the calculation that the result does not critically depend on the number of azimuthal and radial modes included. The calculation using one radial mode for each azimuthal mode, as in Zotter's theory,[10] is already a good approximation.

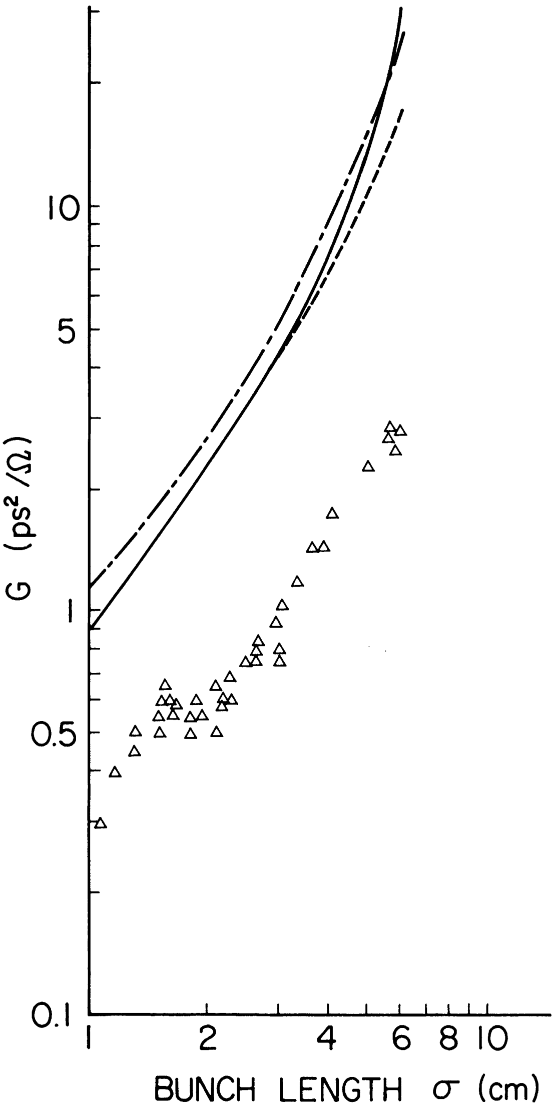

FIGURE 1(a) Scaling parameter G as a function of bunch length σ. The solid curve shows a case where four azimuthal and five radial modes are included. The dashed curve shows a case where two azimuthal and five radial modes are included. The dot-dash curve shows a case where two azimuthal modes and only one radial mode for each azimuthal mode are included. The triangles show the experimental data. The coupling impedance of Wilson et al.[14] is used.

We have also calculated the potential-well bunch lengthening using the coupling impedance of Wilson et al. The bunch lengthening $\Delta\sigma/\sigma$ due to potential-well distortion is given by[18]

$$\frac{\Delta\sigma}{\sigma} = -\frac{\xi e}{2\pi}\sum_{p=1}^{\infty} \mathrm{Im}\, Z(p\omega_0)p\exp(-p^2\sigma^2/2), \tag{3.3}$$

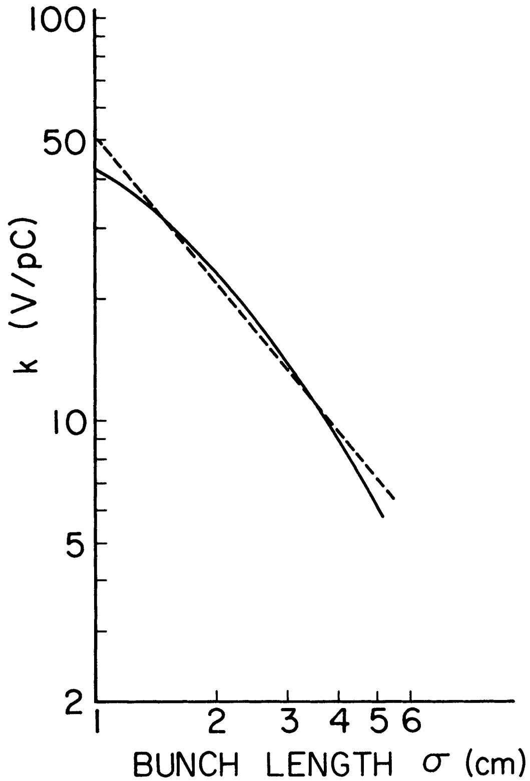

FIGURE 1(b) Loss parameter k as a function of bunch length σ. The solid curve shows the calculation when the same coupling impedance as in Fig. 1(a) is used. The dashed curve represents the experimental data.

where ξ is given by Eq. (2.49). The numerical results are $\Delta\sigma/\sigma = -3.2 \times 10^{-2}$/mA at $\sigma = 1.76$ cm, $\nu_s = 0.033$ and $E = 1.55$ GeV, $\Delta\sigma/\sigma = -6.9 \times 10^{-3}$/mA at $\sigma = 2.51$ cm, $\nu_s = 0.033$ and $E = 2.21$ GeV and $\Delta\sigma/\sigma = -2.4 \times 10^{-3}$/mA at $\sigma = 2.68$ cm, $\nu_s = 0.042$ and $E = 3.0$ GeV. The results are consistent with the experimental data.[14]

Resonator Model

Other parametrizations have been tried and fitted to the experimental data. The simplest parametrization is a broadband resonator model given by

$$Z(\omega) = \frac{R_s}{1 - iQ\left(\dfrac{\omega}{\omega_r} - \dfrac{\omega_r}{\omega}\right)}. \tag{3.4}$$

With this parametrization, the threshold current is fitted. The result is shown in Fig. 2(a). The parameters are $R_s = 4 \times 10^4$ ohm, $Q = 0.6$ and $\omega_r/2\pi = 1.3$ GHz. The calculated curve fits qualitatively well with the experimental data. The wiggle observed at about $\sigma = 1.5$ cm is also reproduced. To see the details of the mode coupling, the

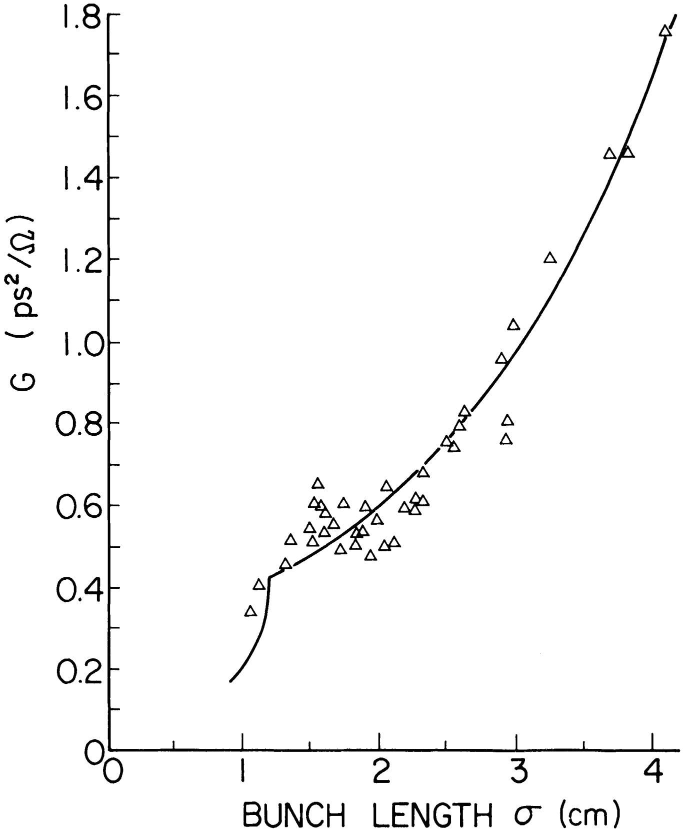

FIGURE 2(a) Scaling parameter G as a function of bunch length σ. The solid curve shows the calculation when a resonator impedance of $R_s = 4 \times 10^4$ ohm, $Q = 0.6$ and $\omega_r/2\pi = 1.3$ GHz is used. The triangles show the experimental data.

real and imaginary parts of the coherent oscillation frequency λ in units of synchrotron frequency are shown in Figs. 3(a) and 3(b) for $\sigma = 0.9$ cm (30 ps) and in Figs. 4(a) and 4(b) for $\sigma = 1.8$ cm (60 ps). For simplicity, two radial modes are shown in the figures. We see that at $\sigma = 0.9$ cm, mode coupling between $m = 1$ and $m = -1$ modes occurs while at $\sigma = 1.8$ cm, mode coupling between $m = 1$ and $m = 2$ modes occurs. We thus see that the wiggle at about $\sigma = 1.5$ cm is explained by the change of the combinations of azimuthal modes in this range of bunch length. The loss parameter k is calculated by using the same impedance as described above and plotted by a solid curve in Fig. 2(b). The fit to the experimental data of Eq. (3.2) is also shown by a dotted curve. The calculated values are larger than the experimental values by factor of about three. Thus the absolute value prediction of theory is not so good, although it explains the qualitative behavior of threshold currents fairly well.

A Further Parametrization of Coupling Impedance

A low-Q resonator model is frequently used to parametrize a broadband impedance. However, in this model, Re $Z(\omega)$ behaves as $1/\omega^2$ and Im $Z(\omega)$ behaves as $1/\omega$ as ω

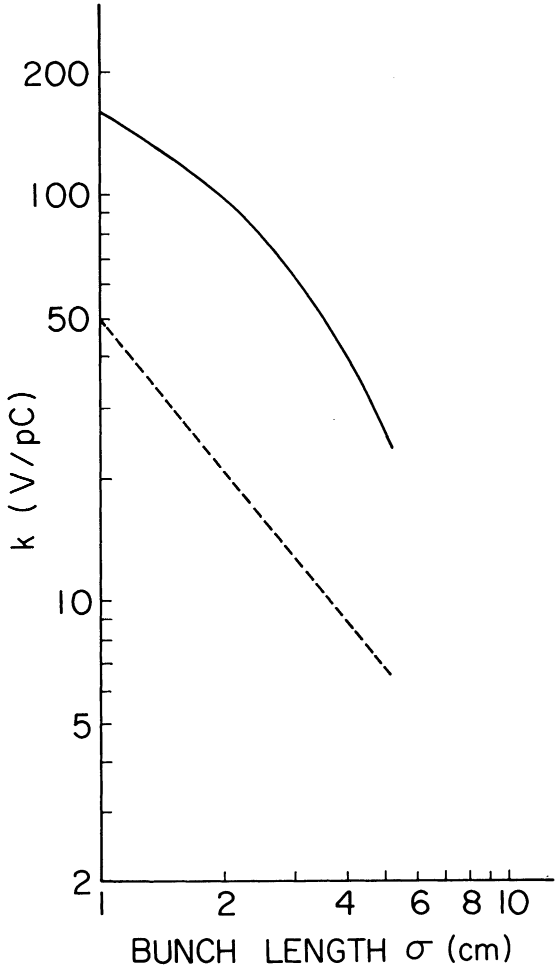

FIGURE 2(b) Loss parameter k as a function of bunch length σ. The solid curve shows the calculation when the same coupling impedance as in Fig. 2(a) is used. The dashed curve represents the experimental data.

becomes large. On the other hand, the scaling law of Chao and Gareyte requires an asymptotic form that Re $Z(\omega)$ and Im $Z(\omega)$ behave as $\omega^{-0.68}$. A simple extension of the resonator model, which has a causal property is given by formula 2.3.2 of Ref. 19.

$$\int_{-\infty}^{\infty} (a - ix)^{-\nu} e^{-ixy}\, dx = \begin{cases} 2\pi y^{\nu-1} e^{-ay}/\Gamma(\nu) & y > 0 \\ 0 & y < 0 \end{cases}$$

$$(\mathrm{Re}\, a > 0, \mathrm{Re}\, \nu > 0). \tag{3.5}$$

With the formula (3.5) we parametrize the coupling impedance as

$$Z(\omega) = \frac{R}{Q} \frac{\omega_s}{2\omega_r} i^\nu \left\{ \frac{\omega_1 \omega_s^{\nu-1}}{(\omega - \omega_1)^\nu} - \frac{\omega_2 \omega_s^{\nu-1}}{(\omega - \omega_2)^\nu} \right\}, \tag{3.6}$$

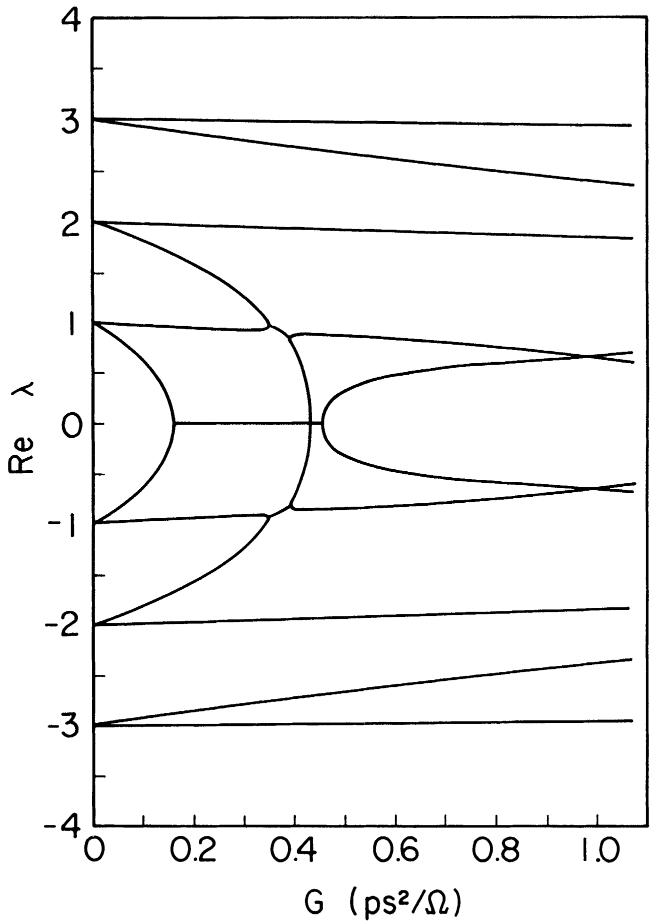

FIGURE 3(a) The real part of the coherent frequency λ in unit of synchrotron frequency as a function of the scaling parameter G. The bunch length is 0.9 cm.

where

$$\omega_1 = \omega_r - i\alpha, \tag{3.7}$$

$$\omega_2 = -\omega_r - i\alpha, \tag{3.8}$$

$$\omega_r = \omega_s\left(1 - \frac{1}{4Q^2}\right)^{1/2}, \tag{3.9}$$

$$\alpha = \frac{\omega_s}{2Q}, \tag{3.10}$$

and the reality condition

$$Z(-\omega) = Z^*(\omega) \tag{3.11}$$

is taken into account. Here the asterisk denotes complex conjugate. For $\nu = 1$, Eq. (3.6)

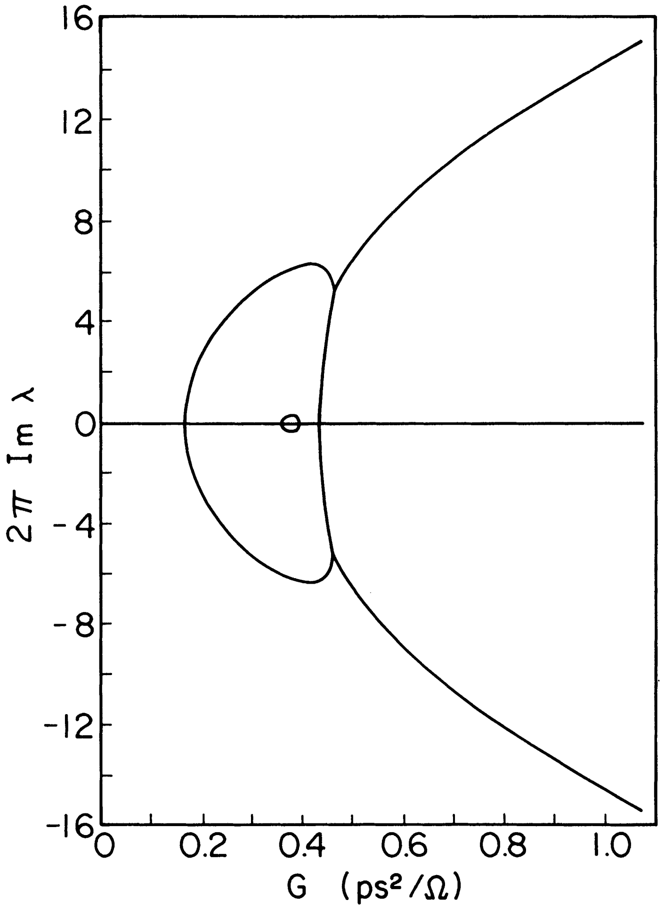

FIGURE 3(b) The imaginary part of 2π times the coherent frequency λ in unit of synchrotron frequency as a function of the scaling parameter G. The bunch length is 0.9 cm.

reduces to a resonator impedance. The wake function $W(t)$ is given by

$$W(t) = \int_{-\infty}^{\infty} Z(\omega)\exp(-i\omega t)\,d\omega$$

$$= \frac{R}{Q}\frac{\omega_s{}^{\nu}}{\omega_r}\frac{2\pi t^{\nu-1}}{\Gamma(\nu)}\{\omega_r\cos\omega_r t - \alpha\sin\omega_r t\}. \tag{3.12}$$

For the impedance of Wilson et al., Bane and Wilson[15] found that Im $Z(\omega)$ goes like $\omega^{-0.68}$ as ω becomes large and Siemann[16] found that the wake function behaves as $t^{-0.32}$ for small t. These properties are nicely reproduced with the impedance (3.6) if we take $\nu = 0.68$.

We have tried to fit the data for bunch lengthening and higher-order mode losses with the impedance (3.6) for $\nu = 0.68$ and variable ν. The result, however, is not much improvement over the resonator model.

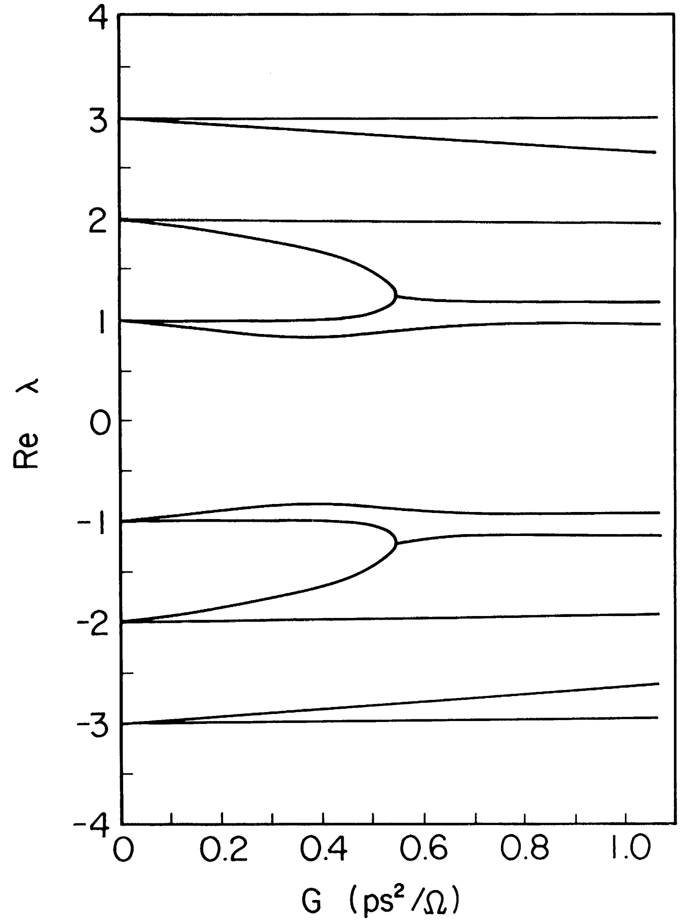

FIGURE 4(a) The real part of the coherent frequency λ in unit of synchrotron frequency as a function of the scaling parameter G. The bunch length is 1.8 cm.

4. CONCLUSIONS

A mode-coupling theory is developed for a Gaussian bunch in which any number of azimuthal and radial modes can be included. It converts Sacherer's integral equation with mode coupling into a matrix eigenvalue problem. It is similar to and closely related to Satoh's theory as described in the Appendix, but it is better suited for computer calculation when many radial modes are included. In addition, the mode eigenfunction can be obtained more easily.

The theory is applied to bunch lengthening in SPEAR II. It explains qualitative features of the experimental data fairly well, but quantitative agreement between the theory and the experiment is not good when we try to explain both the bunch lengthening and the higher-order mode loss with a single coupling impedance. This is partly ascribed to our insufficient knowledge of the coupling impedance. The coupling impedance may have a more complicated form such as the sum of the effects of vacuum chambers, cavities and resistive walls.

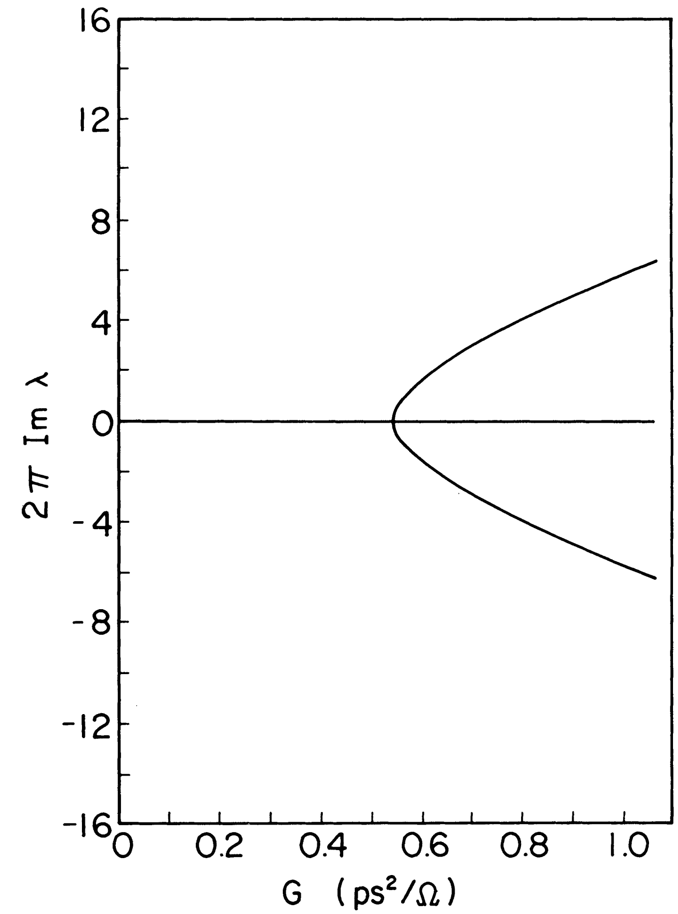

FIGURE 4(b) The imaginary part of the circular coherent frequency $2\pi\lambda$ in unit of synchrotron frequency as a function of the scaling parameter G. The bunch length is 1.8 cm.

Though quantitative agreement is not good, the present theory can provide a qualitative an order-of-magnitude estimate for the threshold current of bunch lengthening. Further, a small number of azimuthal modes are shown to take part in bunch lengthening, at least for short bunch length. It may be that a quantitative theory should include such effects as radiation damping and quantum excitation.

ACKNOWLEDGMENT

The authors wish to thank Prof. T. Nishikawa, Prof. T. Kamei and Prof. Y. Kimura for their interest in this work and continual encouragement.

REFERENCES

1. F. Sacherer, CERN/SI-BR/72-5, Geneva, 1972.
2. F. Sacherer, *IEEE Trans. Nucl. Sci.*, **NS-24,** 1393 (1977).

3. K. Robinson, CEAL-1010, Cambridge, 1964.
4. L. J. Laslett, V. K. Neil and A. M. Sessler, *Rev. Sci. Instrum.*, **32,** 276 (1961).
5. A. W. Chao and J. Gareyte, PEP-224, Stanford, 1976.
6. A. W. Chao, SLAC-PUB-2946, Stanford, 1982.
7. A. Hofmann, K. Hübner and B. Zotter, *IEEE Trans. Nucl. Sci.*, **NS-26,** 3514 (1979).
8. K. Satoh, PEP-Note 361, Stanford, 1981.
9. K. Satoh and Y. Chin, KEK Preprint 82-2, Tsukuba, 1982, and also to be published in *Nucl. Instrum. Methods.*
10. B. Zotter, CERN/ISR-TH/82-10, Geneva, 1982.
11. G. Besnier, *Nucl. Instrum. Methods*, **164,** 235 (1979), also thesis, Univ. de Rennes, 1978.
12. T. Suzuki, Particle Accelerators, **12,** 237 (1982).
13. M. Abramowitz and I. A. Stegun, *Handbook of Mathematical Functions* (Dover, New York, 1965).
14. P. B. Wilson, R. Servranckx, A. P. Sabersky, J. Gareyte, G. E. Fischer, A. W. Chao and M. H. R. Donald, *IEEE Trans. Nucl. Sci.*, **NS-24,** 1211 (1977).
15. K. Bane and P. B. Wilson, PEP-261, Stanford, 1977.
16. R. Siemann, *Nucl. Instrum. Methods*, **203,** 57 (1982).
17. P. B. Wilson, KEK-Accelerator-79-7, Tsukuba, 1980.
18. B. Zotter, CERN/SPS/81-14, Geneva, 1981.
19. A Erdelyi (ed.), *Tables of Integral Transforms*, (McGraw-Hill, New York, 1954) vol. 1. p. 118.

APPENDIX

In this appendix, we will show the relationship between the present theory and Satoh's.[8] The starting point is the eigenvalue equation (2.25), which is rewritten as

$$\frac{m-\lambda}{m} a_h{}^{(m)} = i \frac{e\omega_0}{T\Omega_s C} \sum_{n=-\infty}^{\infty} \sum_{l=0}^{\infty} M_{nl}^{mh} a_l{}^{(n)}. \tag{A.1}$$

With Eqs. (2.26) and (2.27), we can show that $a_h{}^{(m)}$ can be expressed as

$$a_h{}^{(m)} = \frac{m}{m-\lambda} i^m \left\{ \binom{m+2h}{h} \right\}^{1/2} A_{m+2h}(\lambda) \qquad (m > 0), \tag{A.2}$$

where

$$A_{m+2h}(\lambda) = i^{-(m+2h)} \frac{m+2h-\lambda}{m+2h} a_0{}^{(m+2h)}. \tag{A.3}$$

Combining positive and negative m's, we get from Eq. (A.1)

$$b_h{}^{(m)} = i \frac{e\omega_0}{T\Omega_s C} \frac{2m^2}{m^2-\lambda^2} \sum_{n=1}^{\infty} \sum_{l=0}^{\infty} M_{nl}^{mh} b_l{}^{(n)}, \tag{A.4}$$

where

$$b_h{}^{(m)} = a_h{}^{(m)} + a_h{}^{(-m)}. \tag{A.5}$$

From Eq. (A.2), we obtain

$$b_h{}^{(m)} = \frac{2m^2}{m^2-\lambda^2} i^m \left\{ \binom{m+2h}{h} \right\}^{1/2} A_{m+2h}(\lambda). \tag{A.6}$$

If we put

$$I_{mh}(p) = \left\{\binom{m+2h}{h}\right\}^{1/2} F_{m+2}h(p), \tag{A.7}$$

and

$$M_{kl} = \sum_{p=-\infty}^{\infty} \frac{Z(p\omega_0 + \Omega)}{p + \frac{\Omega}{\omega_0}} F_k\left(p + \frac{\Omega}{\omega_0}\right) F_l\left(p + \frac{\Omega}{\omega_0}\right), \tag{A.8}$$

we obtain the matrix equation

$$A_{k'} = -iK \sum_{l'=1}^{\infty} M_{k'l'} A_{l'} \sum_{l'=n+2l} \frac{n^2}{n^2 - \lambda^2} \binom{n+2l}{l}, \tag{A.9}$$

where

$$K = \frac{Ne^2\alpha}{\pi\nu_s{}^2 ET\sigma_\theta{}^2}. \tag{A.10}$$

By putting

$$B_{l'} = A_{l'} \sum_{l'=n+2l} \frac{n^2}{n^2 - \lambda^2} \binom{n+2l}{l}, \tag{A.11}$$

we get the matrix equation of Satoh

$$B_{k'} = -ik\beta_{k'}(\lambda^2) \sum_{l'=1}^{\infty} M_{k'l'} B_{l'}, \tag{A.12}$$

where

$$\beta_k(\lambda^2) = \sum_{k=n+2l} \frac{n^2}{n^2 - \lambda^2} \binom{n+2l}{l}. \tag{A.13}$$

To see the relation of the two theories more closely, we go to the frequency domain. With the expansion (2.22) for $R_m(r)$, the distribution function $\tilde{\rho}_m(p)$ in the frequency domain is given by the Hankel transform of $R_m(r)$ as

$$\begin{aligned}\tilde{\rho}_m(p) &= i^{-m} \int_0^\infty R_m(r) J_m(pr)\, r dr \\ &= \sum_{k=0}^{\infty} a_k{}^{(m)} I_{mk}(p),\end{aligned} \tag{A.14}$$

where Eq. (2.27) is used. With the function $F_{m+2k}(p)$ defined by Eq. (A.7),

$$\tilde{\rho}_m(p) = \sum_{k=0}^{\infty} a_k{}^{(m)} \left\{\binom{m+2k}{k}\right\}^{1/2} F_{m+2k}(p). \tag{A.15}$$

We thus see that different $\tilde{\rho}_m(p)$'s are expanded in terms of the same set of linearly independent functions $\{F_{m+2k}(p)\}$.

Satoh used the sum $\tilde{\rho}(p)$ over the azimuthal modes

$$\tilde{\rho}(p) = \sum_{m=-\infty}^{\infty} \tilde{\rho}_m(p). \tag{A.16}$$

Combining positive and negative m's, we obtain

$$\tilde{\rho}(p) = \sum_{k'=0}^{\infty} F_{k'}(p)\alpha_{k'}, \tag{A.17}$$

where

$$\alpha_{k'} = \sum_{k'=m+2k} i^{-m} \frac{2m}{m+\lambda} a_k^{(m)} \left\{ \binom{k'}{k} \right\}^{1/2}. \tag{A.18}$$

By use of Eq. (A.2), we obtain

$$\begin{aligned} \alpha_{k'} &= \sum_{k'=m+2k} \frac{2m^2}{m^2-\lambda^2} \binom{k'}{k} A_{k'} \\ &= B_{k'}. \end{aligned} \tag{A.19}$$

Thus, $\alpha_{k'}$ in Eq. (A.17), which is the expansion coefficient, is equal to $B_{k'}$ defined by Eq. (A.11).